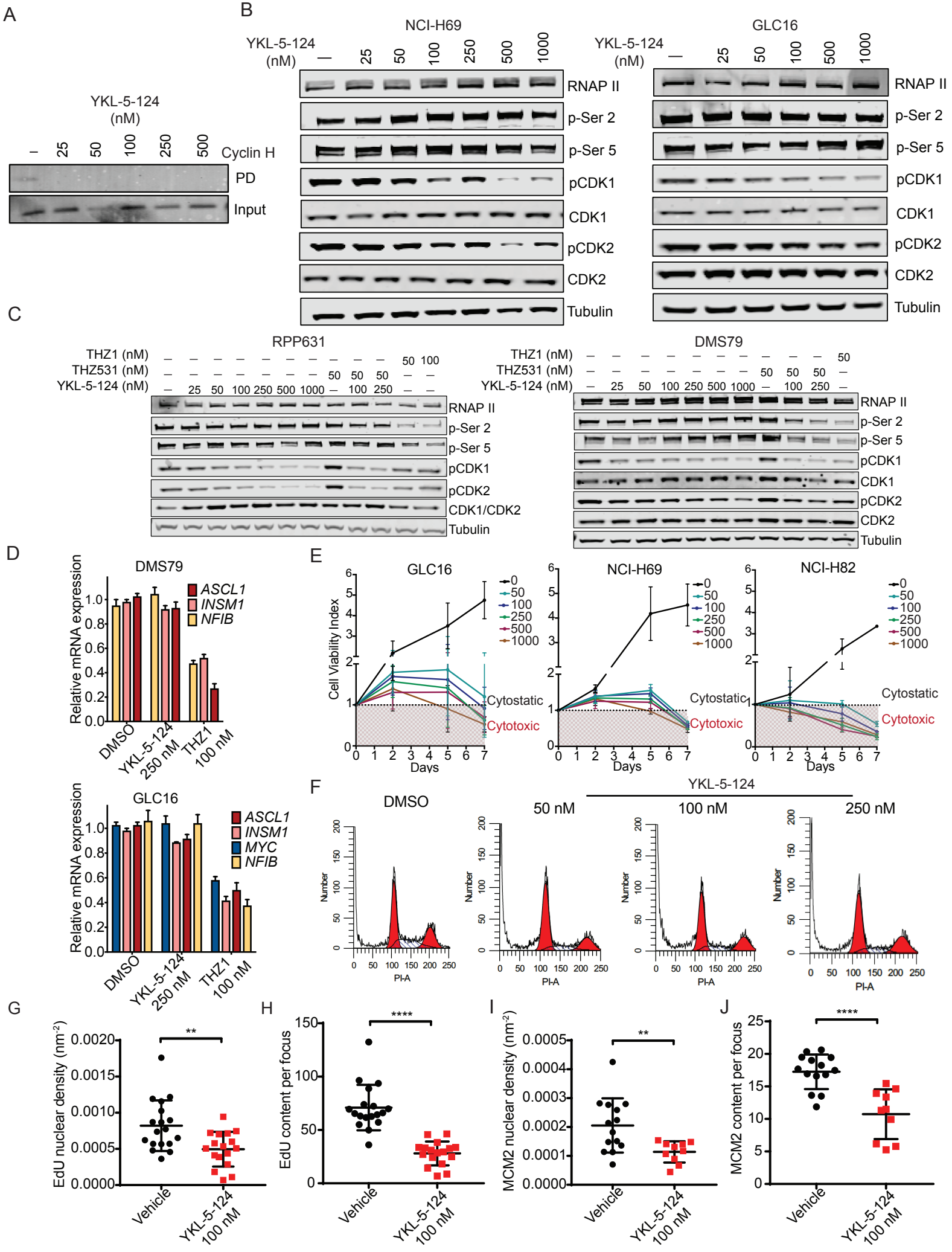
A
YKL-5-124 (nM)
– 25 50 100 250 500
Cyclin H
PD
Input
B
NCI-H69
YKL-5-124 (nM)
— 25 50 100 250 500 1000
GLC16
YKL-5-124 (nM)
— 25 50 100 500 1000
RNAP II
p-Ser 2
p-Ser 5
pCDK1
CDK1
pCDK2
CDK2
Tubulin
C
RPP631
THZ1 (nM)
THZ531 (nM)
YKL-5-124 (nM)
— — — — — — — — — — 50 100
— — — — — — — 50 50 50 — —
— 25 50 100 250 500 1000 — 100 250 — —
CDK1/CDK2
DMS79
THZ1 (nM)
THZ531 (nM)
YKL-5-124 (nM)
— — — — — — — — — — 50
— — — — — — — 50 50 50 —
— 25 50 100 250 500 1000 — 100 250 —
D
DMS79
Relative mRNA expression
ASCL1
INSM1
NFIB
DMSO
YKL-5-124 250 nM
THZ1 100 nM
GLC16
ASCL1
INSM1
MYC
NFIB
E
GLC16
NCI-H69
NCI-H82
Cell Viability Index
0 50 100 250 500 1000
Cytostatic
Cytotoxic
Days
F
DMSO
YKL-5-124
50 nM
100 nM
250 nM
Number
PI-A
G
EdU nuclear density (nm-2)
Vehicle
YKL-5-124 100 nM
H
EdU content per focus
I
MCM2 nuclear density (nm-2)
J
MCM2 content per focus

Figure S1, related to Figure 1 and 2. YKL-5-124 specifically targets CDK7, disrupts cell cycle progression through inhibition of CDK7 CAK activity, and impairs DNA synthesis and MCM2 complex.

(A) Competitive pulldown assay in DMS79 treated with YKL-5-124 at indicated concentrations for 6 hr. Western blotting showing the pulldown (PD) or input (total lysate) of Cyclin H. (B) Western blotting analysis of RNA Pol II total, RNA Pol II p-Ser 2, RNA Pol II p-Ser 5, CDK1 total, CDK2 total, pCDK1 (Thr161), pCDK2 (Thr160) and Tubulin expression in NCI-H69 and GLC16 after treatment with YKL-5-124 at indicated concentrations for 24 hr. (C) Western blotting analysis of RNA Pol II total, RNA Pol II CTD-Ser2, RNA Pol II CTD-Ser5, CDK1 total, CDK2 total, pCDK1 (Thr161), pCDK2 (Thr160) and Tubulin expression in RPP631 and DMS79 after treatment with YKL-5-124, THZ531 or THZ1 at indicated concentrations for 24 hr. (D) RT-qPCR analysis of *INSM1*, *ASCL1*, *NFIB* and *MYC* in DMS79 and GLC16 after indicated treatment for 24 hr. Gene expression was normalized to *GUSB*. The RT-qPCR data were presented as fold changes of gene expression in the test sample compared to the vehicle. (E) Cell viability was measured at indicated time points (normalized to day 0) in GLC16, NCI-H69 and NCI-H82 upon treatment with DMSO (0) or increasing concentrations of YKL-5-124 (nM). (F) Flow cytometry analysis of Propidium Iodide (PI)-staining in DMS79 cells after treatment with DMSO or increasing concentrations of YKL-5-124 for 72 hr. (G and H) Quantification of DNA synthesis indicated by EdU incorporation per nucleus as well as within each replication focus in RPP631 cells treated with vehicle or 100 nM YKL-5-124 after 48 hr. (G) Quantification of EdU nuclear density (nm^{-2}) per nucleus and (H) EdU content per focus are plotted. (I and J) Quantification MCM2 complex per nucleus as well as within each replication focus in RPP631 cells treated with vehicle or 100 nM YKL-5-124 after 48 hr. (I) Quantification of MCM2 nuclear density (nm^{-2}) per nuclei and (J) Relative MCM2 content per focus are plotted. (D, E, G, H, I, J) Data shown as means ± SD of three independent experiments run in triplicates. (G, H, I, J) Unpaired two-tailed t-test. **$p < 0.01$, ****$p < 0.0001$.

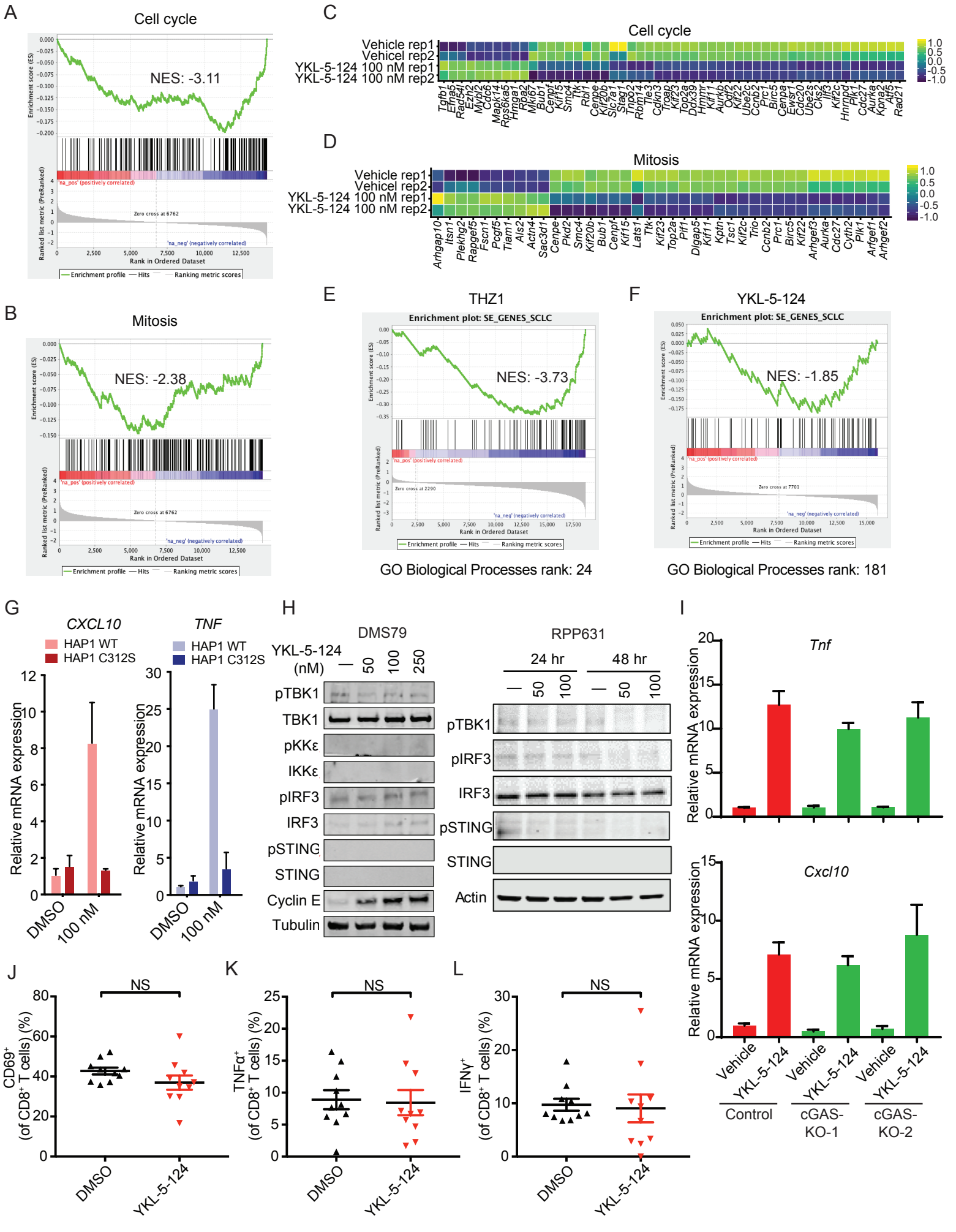
A
Cell cycle
NES: -3.11
B
Mitosis
NES: -2.38
C
Cell cycle
Vehicle rep1
Vehicel rep2
YKL-5-124 100 nM rep1
YKL-5-124 100 nM rep2
D
Mitosis
Vehicle rep1
Vehicel rep2
YKL-5-124 100 nM rep1
YKL-5-124 100 nM rep2
E
THZ1
Enrichment plot: SE_GENES_SCLC
NES: -3.73
GO Biological Processes rank: 24
F
YKL-5-124
Enrichment plot: SE_GENES_SCLC
NES: -1.85
GO Biological Processes rank: 181
G
CXCL10
TNF
HAP1 WT
HAP1 C312S
Relative mRNA expression
DMSO
100 nM
H
DMS79
YKL-5-124 (nM)
pTBK1
TBK1
pKKε
IKKε
pIRF3
IRF3
pSTING
STING
Cyclin E
Tubulin
RPP631
24 hr
48 hr
Actin
I
Tnf
Cxcl10
Relative mRNA expression
Vehicle
YKL-5-124
Control
cGAS-KO-1
cGAS-KO-2
J
CD69+ (of CD8+ T cells) (%)
NS
K
TNFα+ (of CD8+ T cells) (%)
L
IFNγ+ (of CD8+ T cells) (%)

Figure S2, related to Figure 3. YKL-5-124 disrupts cell cycle and induces pro-inflammatory cytokine/chemokine production.

(A and B) GSEA analysis of the differentially expressed genes induced by YKL-5-124 in RPP631. Here shown are two of the top most negatively regulated 'Hallmarks' signatures. Gene list was ranked with signed (from $\log_2$ fold change (FC)) likelihood ratio from YKL-5-124 versus vehicle comparison. (C and D) Heatmaps for differential expression of transcripts from two top negatively regulated pathways in GSEA analysis between vehicle and YKL-5-124 treated cells (colors are $\log_2$FC). (E and F) GSEA analysis of expressed genes associated with super enhancers (SEs) induced by (E) THZ1 (Christensen et al., 2014) or (F) YKL-5-124 in SCLC. Ranking of SE-genes enrichment was compared to all GO Biological Processes gene sets in each dataset. (G) RT-qPCR analysis of *TNF* and *CXCL10* in HAP1 CDK7 WT and HAP1 CDK7 C312S cells after treatment with DMSO or 100 nM YKL-5-124 for 48 hr. The RT-qPCR data were presented as fold changes of gene expression compared to the vehicle. (H) Western blotting analysis of the STING-TBK1-IRF3 pathway in YKL-5-124-treated DMS79 and RPP631. (I) RT-qPCR analysis of *Tnf* and *Cxcl10* levels upon 48 hr YKL-5-124 treatment in the CRISPR/Cas9 cGAS knockout (KO) RPP631 cells. The RT-qPCR data were presented as fold changes of gene expression compared to the vehicle. (J-L) Profiling of OT-I $CD8^+$ T cells by flow cytometry analysis after treatment with DMSO or YKL-5-124. T cell activity markers (J) CD69, (K) TNFα and (L) IFNγ were examined. (G, I) Data shown as means $\pm$ SD of three independent experiments run in triplicates. (J, K, L) Data shown as means $\pm$ SEM of three independent experiments run in ten replicates. Unpaired two-tailed t-test. NS, not significant.

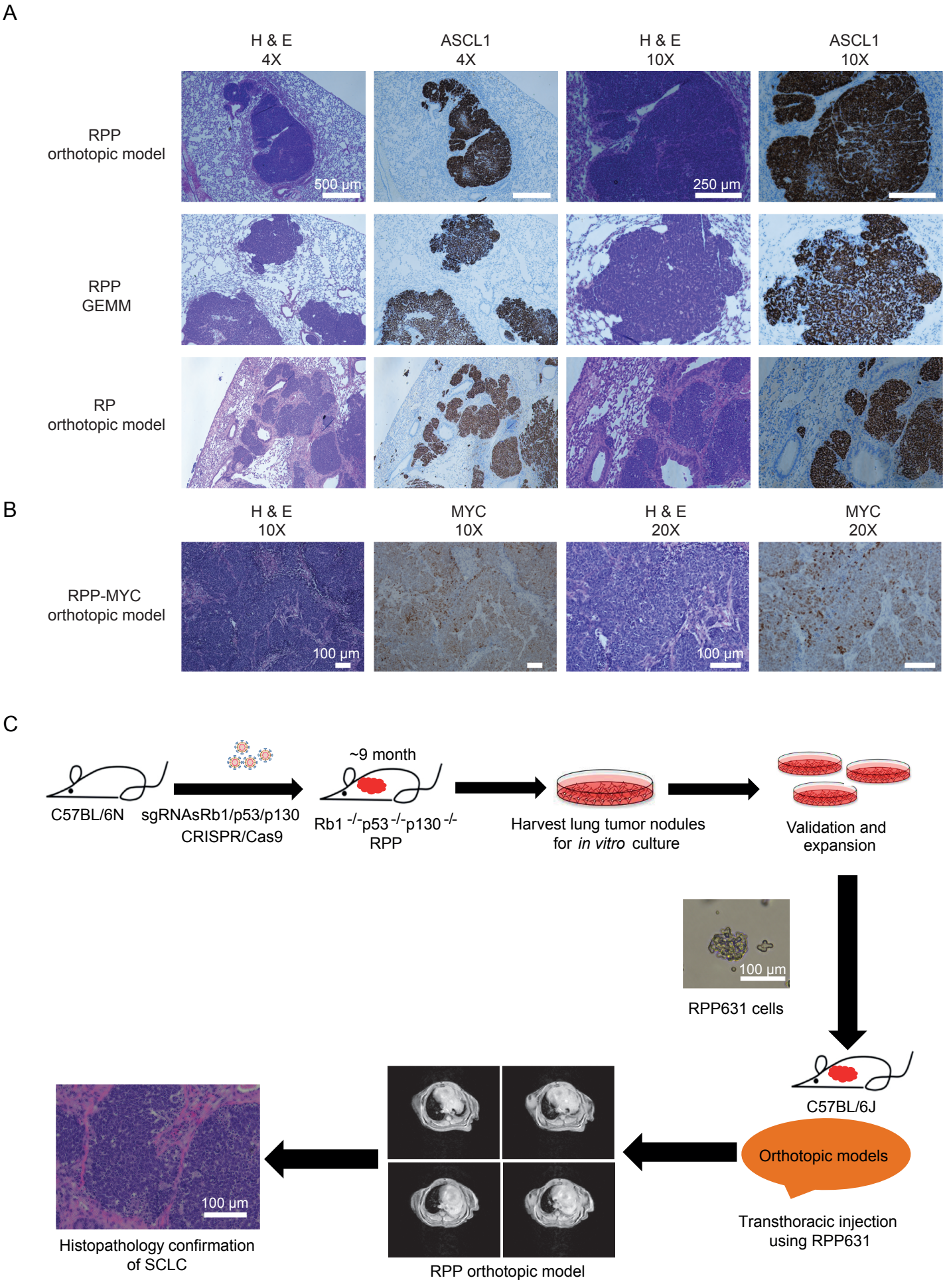
A
H & E
4X
ASCL1
4X
H & E
10X
ASCL1
10X
RPP
orthotopic model
RPP
GEMM
RP
orthotopic model
500 µm
250 µm
B
H & E
10X
MYC
10X
H & E
20X
MYC
20X
RPP-MYC
orthotopic model
100 µm
100 µm
C
C57BL/6N
sgRNAsRb1/p53/p130
CRISPR/Cas9
~9 month
Rb1 -/-p53 -/-p130 -/-
RPP
Harvest lung tumor nodules
for in vitro culture
Validation and
expansion
100 µm
RPP631 cells
C57BL/6J
Orthotopic models
Transthoracic injection
using RPP631
RPP orthotopic model
100 µm
Histopathology confirmation
of SCLC

Figure S3, related to Figure 4. Histopathology of murine SCLC models and establishment of syngeneic mouse models for studying oncoimmunology in SCLC.

(A) Representative images of H & E and immunohistochemistry (IHC) staining for ASCL1 of lung tumors from RPP GEMM, RPP and RP orthotopic models as indicated. (B) Representative images of H & E and IHC staining for MYC of lung tumors from RPP-MYC orthotopic model. (C) Experimental approach of establishing RPP orthotopic model. Using *in vivo* CRISPR/Cas9-mediated loss-of-function gene editing, single-guide RNAs (sgRNAs) designed to inactivate tumor suppressors *Rb1*, *p53* and *p130* were delivered through intratracheal induction into mouse lung to generate a murine SCLC model. After 9 months, lung tumor nodules were harvested for *in vitro* culture. Established RPP631 cells were injected back to C57BL/6 background mice orthotopically. Tumor burden was monitored by MRI and histopathology of SCLC was confirmed by rodent pathologist.

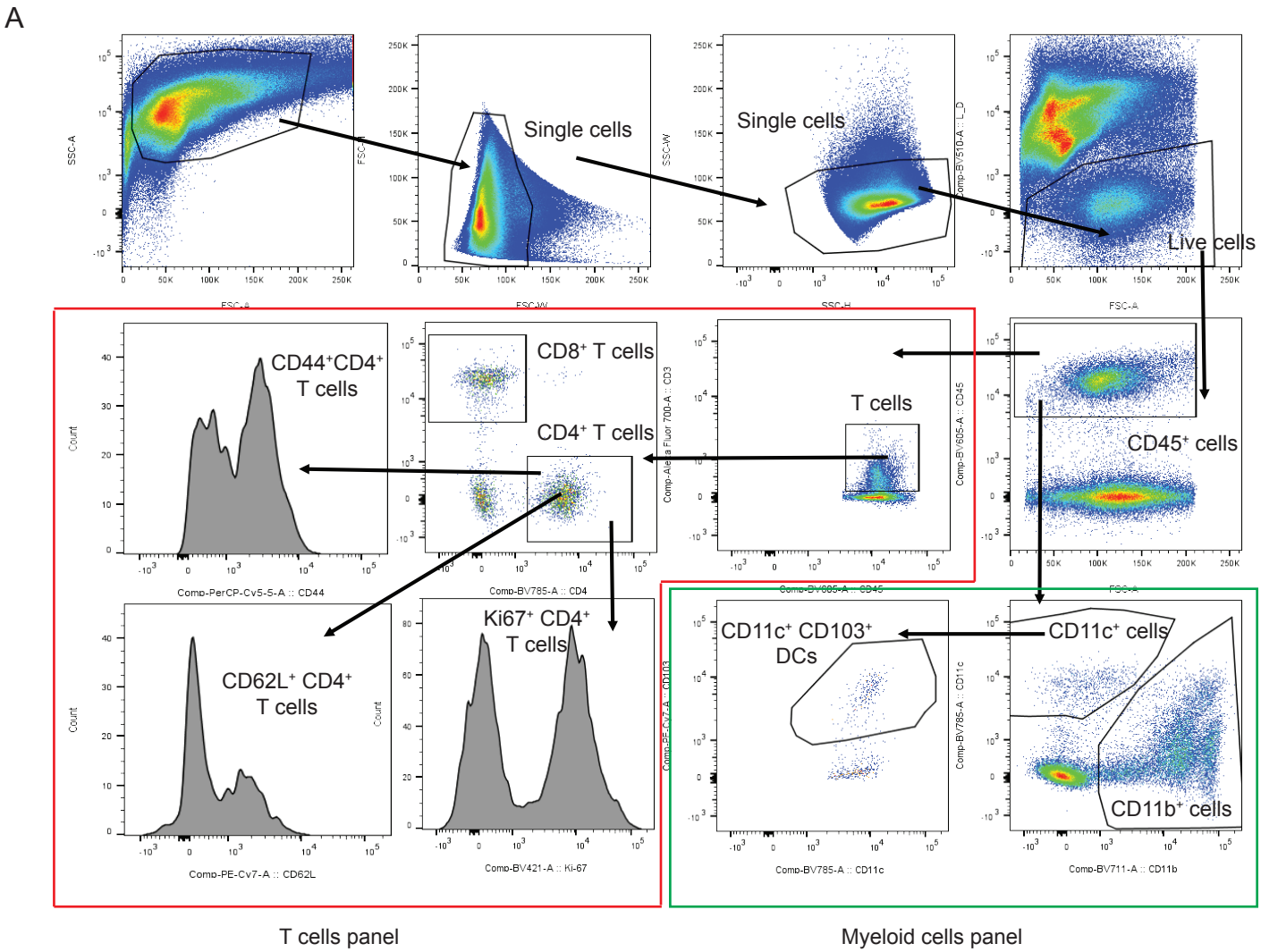
A
Single cells
Single cells
Live cells
CD44⁺CD4⁺ T cells
CD8⁺ T cells
CD4⁺ T cells
T cells
CD45⁺ cells
CD62L⁺ CD4⁺ T cells
Ki67⁺ CD4⁺ T cells
CD11c⁺ CD103⁺ DCs
CD11c⁺ cells
CD11b⁺ cells
T cells panel
Myeloid cells panel

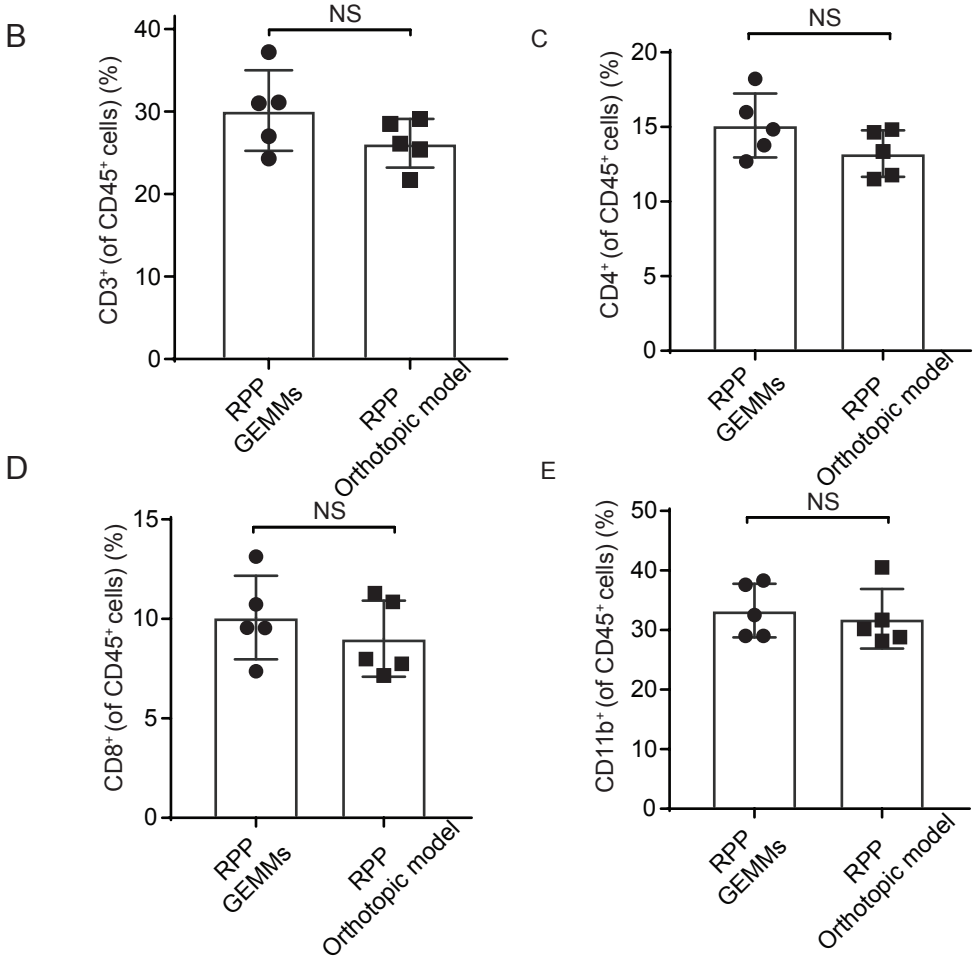
B
NS
CD3⁺ (of CD45⁺ cells) (%)
RPP GEMMs
RPP Orthotopic model
C
NS
CD4⁺ (of CD45⁺ cells) (%)
RPP GEMMs
RPP Orthotopic model
D
NS
CD8⁺ (of CD45⁺ cells) (%)
RPP GEMMs
RPP Orthotopic model
E
NS
CD11b⁺ (of CD45⁺ cells) (%)
RPP GEMMs
RPP Orthotopic model

Figure S4, related to Figure 4. Immune profiling gating strategy and comparison of the TME in RPP orthotopic syngeneic model versus GEMM model

(A) Representation of an example of gating strategy. Single cells were first gated and followed by aqua live/dead staining selection for live cells. Total immune cells were identified by CD45 staining. A sequential gating strategy was then used to identify various populations using specific markers: total T cells ($CD3^+$), $CD4^+$ T cells, $CD8^+$ T cells, myeloid cells ($CD11b^+$), and dendritic cells ($CD11c^+CD103^+$). In addition, the expression of CD44, CD62L and Ki67 in $CD4^+$ T cells was analyzed. (B-E) Tumor infiltrating lymphocytes from tumor-bearing lung in the RPP orthotopic syngeneic model and RPP GEMM were analyzed by flow cytometry when tumor sizes were comparable. (B) Total T cells ($CD45^+CD3^+$), (C) $CD4^+$ T cells, (D) $CD8^+$ T cells and (E) myeloid cells ($CD11b^+$) were quantified and compared. Data shown as means ± SD. Unpaired two-tailed t-test. NS, not significant.

A

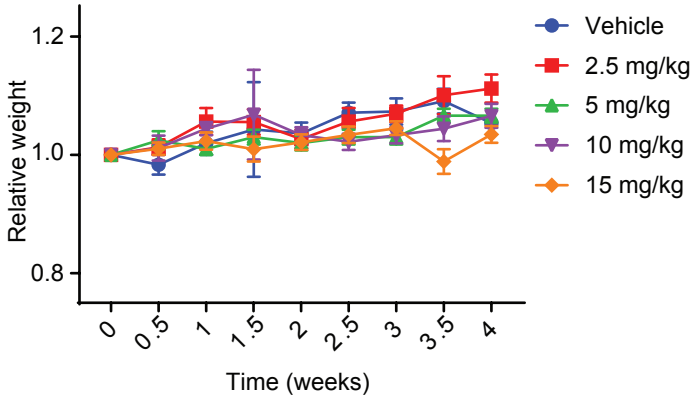
Relative weight
1.2
1.0
0.8
0
0.5
1
1.5
2
2.5
3
3.5
4
Time (weeks)
Vehicle
2.5 mg/kg
5 mg/kg
10 mg/kg
15 mg/kg

B

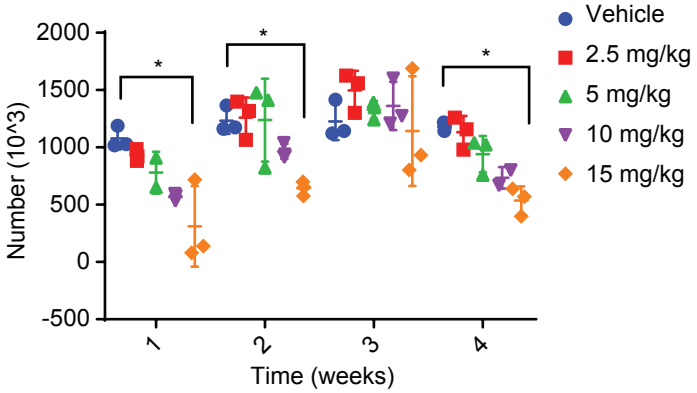
Number (10^3)
2000
1500
1000
500
0
-500
*
*
*
1
2
3
4
Time (weeks)
Vehicle
2.5 mg/kg
5 mg/kg
10 mg/kg
15 mg/kg

C

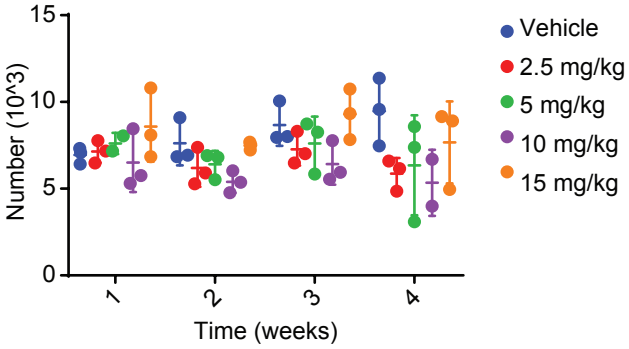
Number (10^3)
15
10
5
0
1
2
3
4
Time (weeks)
Vehicle
2.5 mg/kg
5 mg/kg
10 mg/kg
15 mg/kg

D

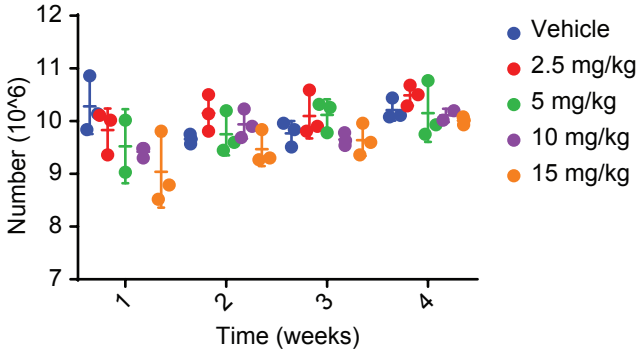
Number (10^6)
12
11
10
9
8
7
1
2
3
4
Time (weeks)
Vehicle
2.5 mg/kg
5 mg/kg
10 mg/kg
15 mg/kg

E

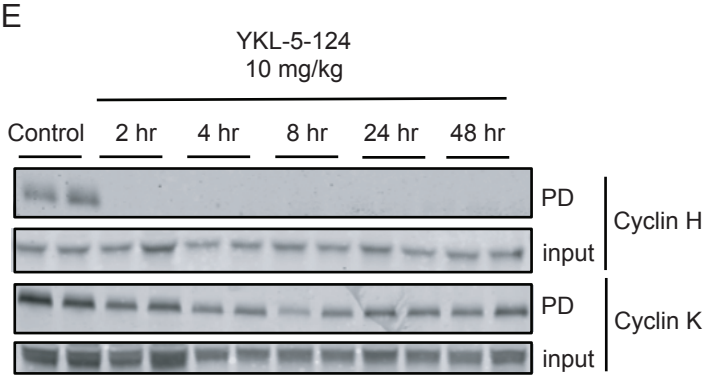
YKL-5-124
10 mg/kg
Control
2 hr
4 hr
8 hr
24 hr
48 hr
PD
input
Cyclin H
PD
input
Cyclin K

Figure S5, related to Figure 4. *In vivo* evaluation of YKL-5-124 treatment toxicity and target engagement.

(A-D) *In vivo* examination of YKL-5-124 treatment toxicities. (A) Body weight and blood cell counts including (B) platelet, (C) white blood cells (WBC) and (D) red blood cells (RBC) were monitored and measured on a weekly basis. Data shown as means ± SD. Unpaired two-tailed t-test. *$p < 0.01$. (E) *In vivo* target engagement of YKL-5-124 by competitive pulldown assay. Tumor-bearing mice were administered with three dosages of YKL-5-124 (10 mg/kg) and tumor tissues were harvested after the last dose at indicated time points. Western blotting showing the pulldown (PD) or input (total lysate) of Cyclin H and Cyclin K.

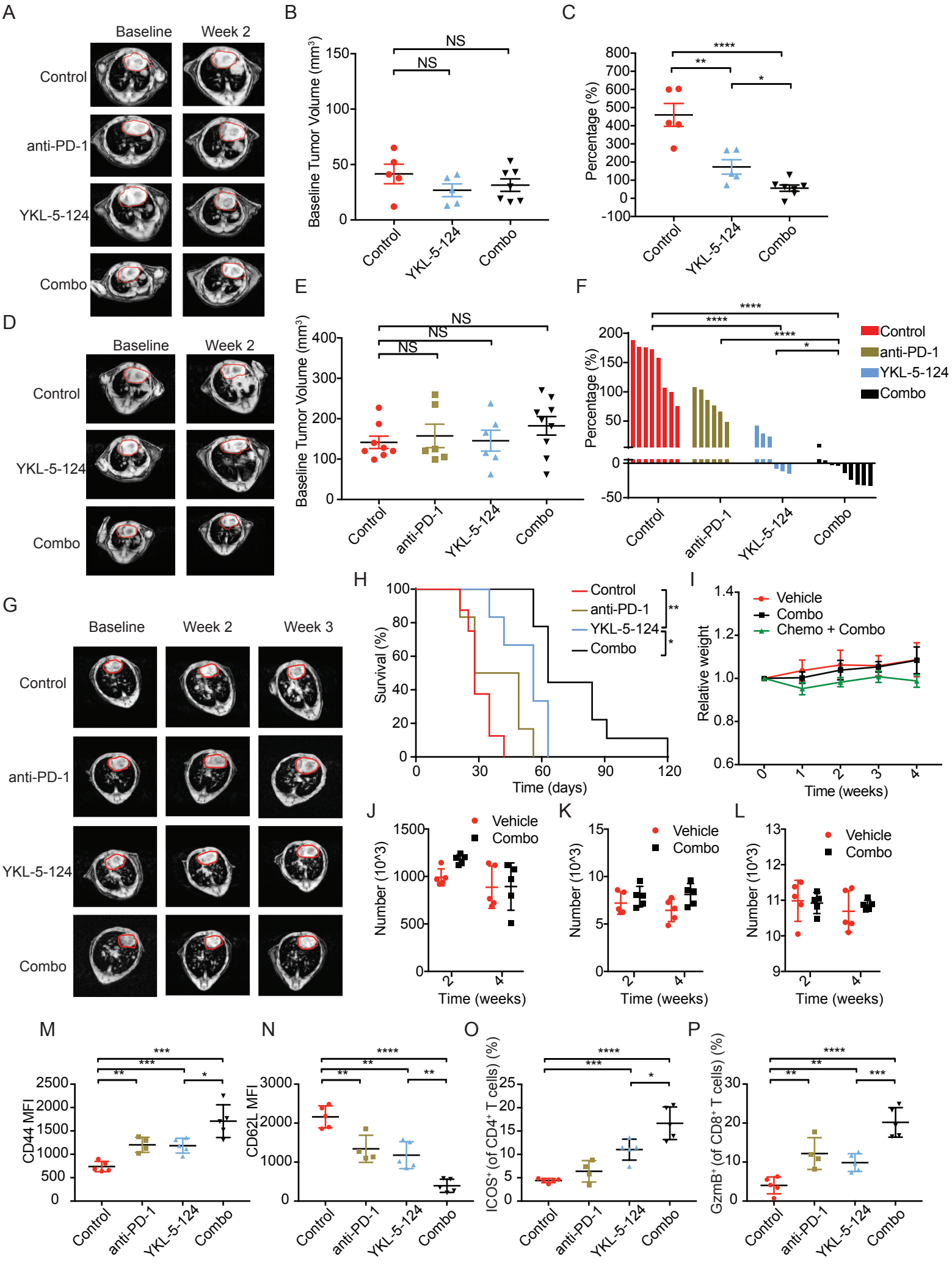
A
Baseline
Week 2
Control
anti-PD-1
YKL-5-124
Combo
B
Baseline Tumor Volume (mm3)
NS
NS
Control
YKL-5-124
Combo
C
Percentage (%)
****
**
*
Control
YKL-5-124
Combo
D
Baseline
Week 2
Control
YKL-5-124
Combo
E
Baseline Tumor Volume (mm3)
NS
NS
NS
Control
anti-PD-1
YKL-5-124
Combo
F
Percentage (%)
****
****
****
*
Control
anti-PD-1
YKL-5-124
Combo
G
Baseline
Week 2
Week 3
Control
anti-PD-1
YKL-5-124
Combo
H
Survival (%)
Control
anti-PD-1
YKL-5-124
Combo
**
*
Time (days)
I
Relative weight
Vehicle
Combo
Chemo + Combo
Time (weeks)
J
Number (10^3)
Vehicle
Combo
Time (weeks)
K
Number (10^3)
Vehicle
Combo
Time (weeks)
L
Number (10^3)
Vehicle
Combo
Time (weeks)
M
CD44 MFI
***
***
**
*
Control
anti-PD-1
YKL-5-124
Combo
N
CD62L MFI
****
**
**
**
Control
anti-PD-1
YKL-5-124
Combo
O
ICOS+ (of CD4+ T cells) (%)
****
***
*
Control
anti-PD-1
YKL-5-124
Combo
P
GzmB+ (of CD8+ T cells) (%)
****
**
**
***
Control
anti-PD-1
YKL-5-124
Combo

Figure S6, related to Figure 4 and Figure 5. YKL-5-124 inhibits tumor growth and enhances tumor response to anti-PD-1 immunotherapy in multiple murine SCLC models.

(A) Representative MRI images show mouse lung tumors before and after the treatment at indicated time points in the RP orthotopic model. Circled areas, heart. (B) Quantification of baseline tumor volumes by MRI scan of RPP-MYC mice. Control group (n= 5), YKL-5-124 (n= 5), Combo (n= 7). (C) Quantification of tumor volume changes by MRI scan of RPP-MYC mice. Each dot represents one mouse, comparing to baseline MRI measurement. (D) Representative MRI images show mouse lung tumors before and after the treatment at indicated time points in the RPP-MYC model. Circled areas, heart. (E) Quantification of baseline tumor volumes by MRI scan of RPP GEMMs. Control group (n= 8), anti-PD-1 (n= 6), YKL-5-124 (n= 6), Combo (n= 9). Each dot represents one mouse. NS, not significant. (F) Quantification of tumor volume changes by MRI scan of RPP GEMMs after treatment with Control, anti-PD-1, YKL-5-124 and Combo. Waterfall plot shows tumor volumes response to the treatment after week 3. Each column represents one mouse, comparing to baseline MRI measurement. (G) Representative MRI images show mouse lung tumors before and after the treatment at indicated time points in the RPP GEMMs. Circled areas, heart. (H) Kaplan-Meier survival curve of RPP GEMMs after indicated treatment. Log-rank test *$p < 0.05$, **$p < 0.01$. (I-L) *In vivo* examination of Combo and Chemo + Combo treatment toxicities (n= 5). (I) Relative body weight and blood cell counts including (J) platelet, (K) WBC, (L) RBC were monitored as shown. (M-P) The expression of CD44, CD62L, Ki67 and ICOS in infiltrating $CD4^+$ T cells after indicated treatment in the RPP GEMMs was analyzed by flow cytometry. MFI of (M) CD44, (N) CD62L and (O) frequency of $ICOS^+$ $CD4^+$ T cells were plotted. (P) The expression of GzmB in infiltrating $CD8^+$ T cells after indicated treatment was analyzed. Frequencies of $GzmB^+$ $CD8^+$ T cells were presented. (B, C, E) Data shown as means ± SEM. (I, J, K, L, M, N, O, P) Data shown as means ± SD. (B, C, E, F, M, N, O, P) Unpaired two-tailed t-test. *$p < 0.05$, **$p < 0.01$, ***$p < 0.001$, ****$p < 0.0001$. NS, not significant.

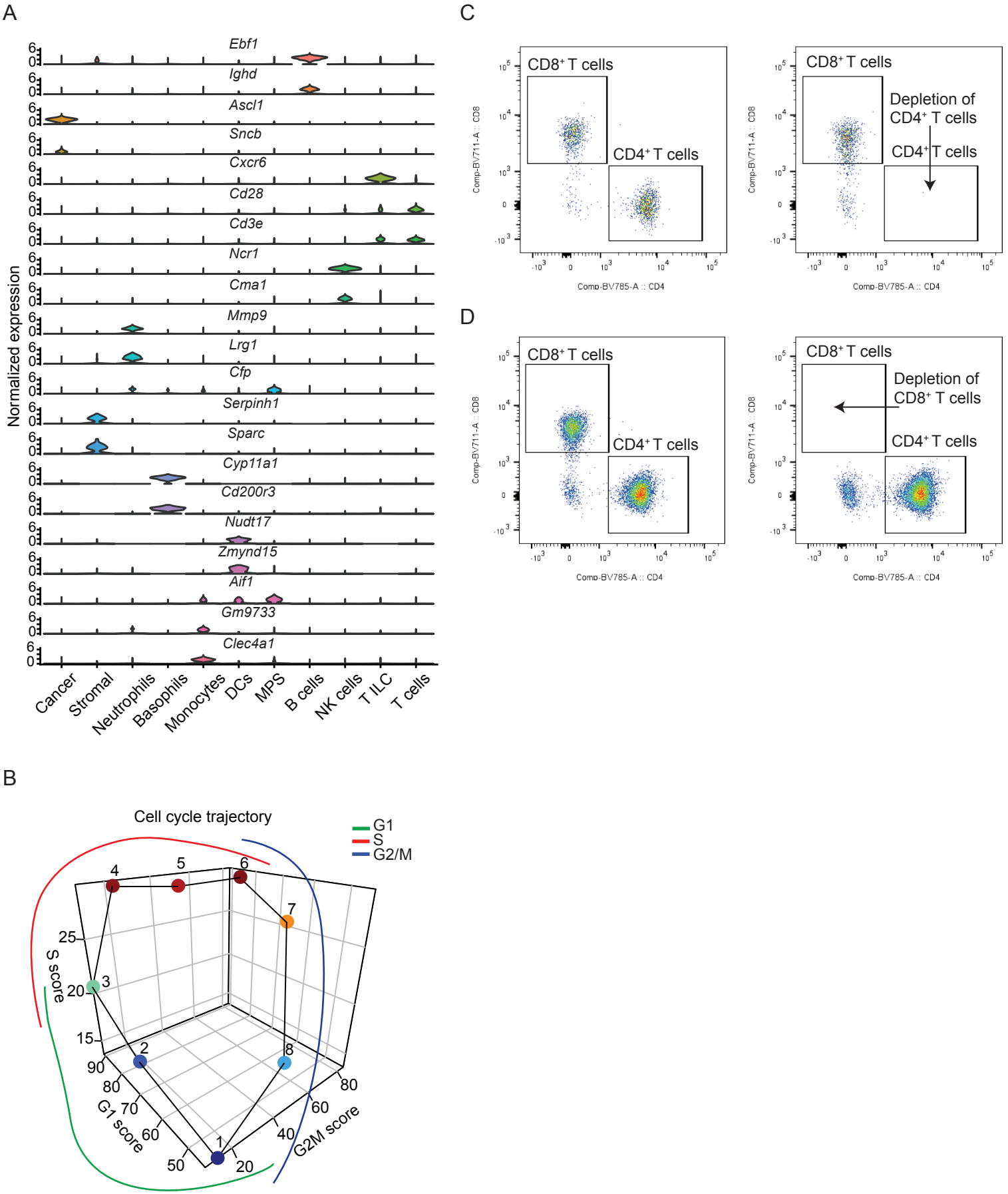
A
Ebf1
Ighd
Ascl1
Sncb
Cxcr6
Cd28
Cd3e
Ncr1
Cma1
Mmp9
Lrg1
Cfp
Serpinh1
Sparc
Cyp11a1
Cd200r3
Nudt17
Zmynd15
Aif1
Gm9733
Clec4a1
Normalized expression
Cancer
Stromal
Neutrophils
Basophils
Monocytes
DCs
MPS
B cells
NK cells
T ILC
T cells
B
Cell cycle trajectory
G1
S
G2/M
S score
G1 score
G2M score
C
CD8⁺ T cells
CD4⁺ T cells
Depletion of CD4⁺ T cells
Comp-BV711-A :: CD8
Comp-BV785-A :: CD4
D
CD8⁺ T cells
CD4⁺ T cells
Depletion of CD8⁺ T cells
Comp-BV711-A :: CD8
Comp-BV785-A :: CD4

Figure S7, related to Figure 6 and 7. Single-cell analysis identifies intratumoral cell populations and confirms connection of CDK7 inhibition in tumor intrinsic signaling to immunity.

(A) Violin plots showing the gene expression distribution of representative markers in each identified cell type. (B) A 3D cell cycle trajectory showing eight clusters of cells at different cell-cycle state based on calculated scores for genes specific to the G1, S and G2/M phase. (C and D) Flow cytometry was performed using splenocytes from mice under αCD4 or αCD8 treatment. (C) Representative density plot showing $CD4^+$ T cell population in control (left) and αCD4 (right) group. (D) Representative density plot showing $CD8^+$ T cell population in control (left) and αCD8 (right) group.